High-frequency electron-spin-resonance measurements on $Mn_x Mg_{1-x} O$ ($x = 1.0\times10^{-4}$) and DPPH at very low temperatures

IOP Conf. Series: Journal of Physics: Conf. Series **969** (2018) 012111 doi:10.1088/1742-6596/969/1/012111

High-frequency electron-spin-resonance measurements on $Mn_xMg_{1-x}O$ ($x = 1.0 \times 10^{-4}$) and DPPH at very low temperatures

Y Ishikawa[1], K Ohya[2], S Miura[1], Y Fujii[2], S Mitsudo[2], T Mizusaki[2], A Fukuda[3], A Matsubara[4], H Kikuchi[1], T Asano[1], H Yamamori[5], S Lee[6] and S Vasiliev[7]

[1] Department of Applied Physics, University of Fukui, Fukui 910-8507, Japan
[2] Research Center for Development of Far-Infrared Region, University of Fukui, Fukui 910-8507, Japan
[3] Department of Physics, Hyogo College of Medicine, Nishinomiya 663-8501, Japan
[4] Department of Physics, Kyoto University, Kyoto 606-8501, Japan
[5] Technical Division, School of Engineering, University of Fukui, Fukui 910-8507, Japan
[6] Department of Physics, Korea Advanced Institute of Science and Technology, Daejeon 305-701, Korea
[7] Department of Physics and Astronomy, University of Turku, Turku 20014, Finland

E-mail: yuya-i@u-fukui.ac.jp

Abstract. We have developed a millimeter-wave electron-spin-resonance (ESR) system for very low temperatures (T < 1 K) that can be employed for nuclear-magnetic-resonance measurements by using dynamic nuclear polarization. The system uses a Fabry-Pérot resonator that works in the frequency range of 125 – 130 GHz and covers the temperature range of 0.09 – 6.5 K. We have performed ESR measurements in the frequency around 128 GHz by using $Mn_xMg_{1-x}O$ ($x = 1.0 \times 10^{-4}$) and free-radical samples of 1, 1-diphenyl-2-picrylhydrazyl (DPPH), because these samples have been proposed as field and sensitivity markers. Temperature dependence of the ESR signal intensity for $Mn_xMg_{1-x}O$ shows anomalies originating from magnetic order are found around 3.5 – 4 K. We estimate the sensitivity of the system for ESR detections to be 6×10^{13} spins/G at 5.8 K. Because DPPH shows no observable shift in the magnetic field, we propose it as a useful standard marker for ESR measurements at very low temperatures.

1. Introduction

Magnetic-resonance techniques such as electron spin resonance (ESR) and nuclear magnetic resonance (NMR) are used in several research fields to provide useful information about the microscopic properties of various material samples. Dynamic nuclear polarization (DNP), in which a high electron-spin polarization is transferred to nuclear polarization through a hyperfine interaction, is a powerful technique for enhancing the sensitivity of NMR measurements. A typical example of DNP was suggested more than 50 years ago in silicon lightly doped with phosphorus (Si:P) [1]. However, it has been difficult to observe the ^{31}P-NMR signal directly, because the critical concentration of P atoms in an insulator is too low. Moreover, recently it becomes intriguing to study spin dynamics, including DNP phenomena, for Si:P at mK temperatures because one of the most practical quantum computer

designs proposed by Kane [2] uses Si:P at high magnetic-field strengths ($B > 3$ T) and low temperatures ($T < 100$ mK). Song *et al*. reported that ^{31}P nuclear-spin polarization is enhanced by two or three orders of magnitude over the thermal-equilibrium value by using DNP induced by microwave irradiation above 80 GHz [3]. Fujii *et al*. have performed steady-state ESR experiments on the donor-electron spin in lightly doped Si:P (concentration $n = 6.5 \times 10^{16}$ cm^{-3}) at 3.6 T and 1.44 K. Their work indicates that the nuclear polarization can be changed by NMR pulse [4]. Recently, Järvinen *et al*. have performed extensive high-frequency ESR studies with a ^{3}He/^{4}He dilution refrigerator (D/R) and have demonstrated ^{31}P nuclear polarization of higher than 98% [5, 6]. We have been developing an ESR/NMR double-magnetic-resonance system enclosed in a D/R probe, which enables us to perform DNP-NMR and ENDOR measurements to investigate ^{31}P spin dynamics. Developments for millimeter-wave ESR devices optimized for operation well below one Kelvin have been challenging and applied to, for example, studies on magnetic systems [7, 8]. In this paper, we report the current status of our developmental work and provide ESR measurements on $Mn_xMg_{1-x}O$ ($x = 1.0 \times 10^{-4}$) and DPPH. We have also determined the ESR sensitivity from measurements on $Mn_xMg_{1-x}O$ and have investigated the behavior of DPPH as a magnetic-field marker at very low temperatures.

2. Experiment

Figure 1 shows a schematic of our ESR apparatus in a ^{3}He/^{4}He D/R (Kelvinox MX 400, Oxford Instruments). The D/R is installed in an 18-T superconducting magnet. A Gunn diode (PLO-6-128-01, Farran Technology) is used as an phase-locked oscillator with the output power of 10 mW around the

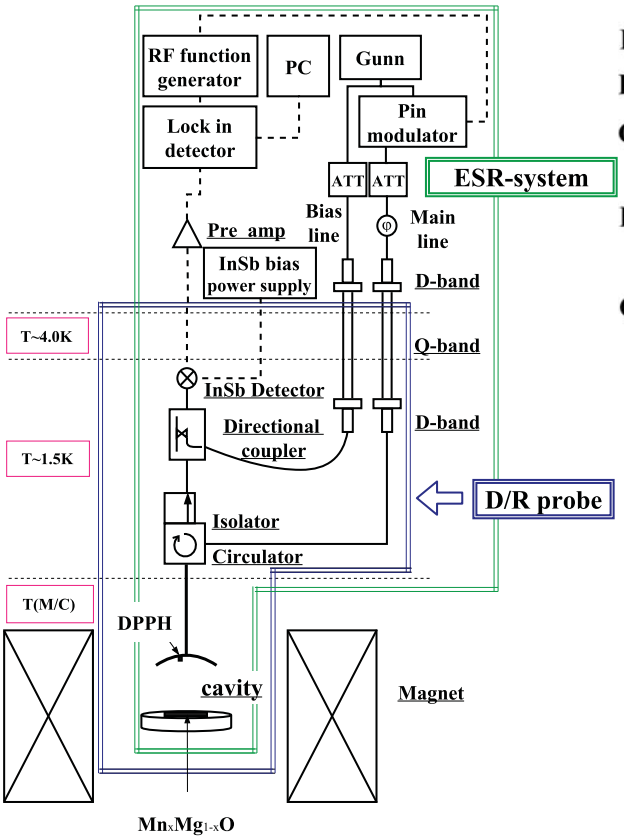

Figure 1. ESR system in the dilution refrigerator used for $Mn_xMg_{1-x}O$ and DPPH measurements.

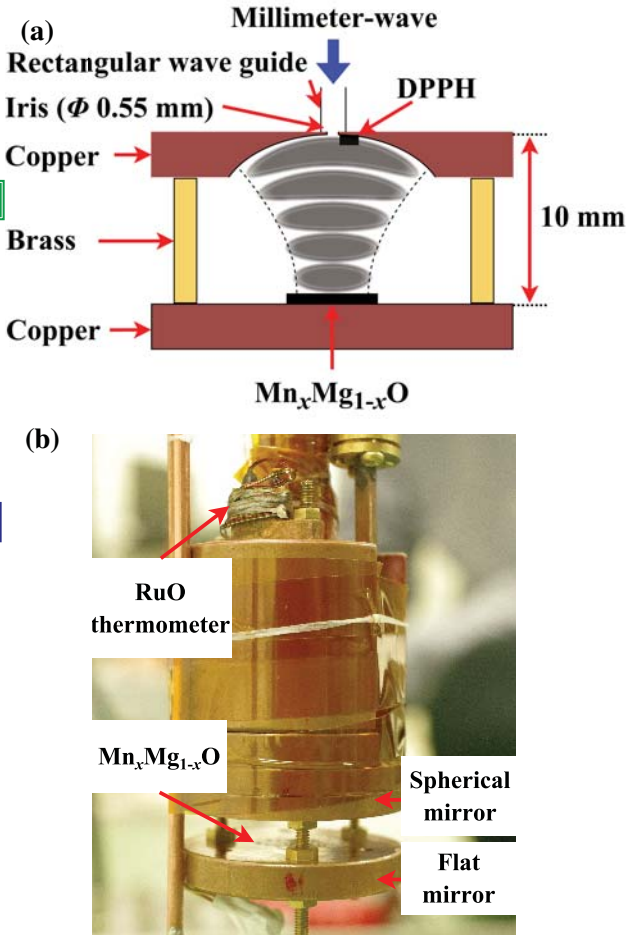

Figure 2. (a) Cross-section of the Fabry-Pérot resonator for our mm-wave ESR. **(b)** A photograph of the Fabry-Pérot resonator.

central frequency (~128 GHz). Millimeter waves from the oscillator are split by a directional coupler into main- and bias-lines in a homodyne detection system at cryogenic temperatures. ATT in Figure 1 stands attenuator. Temperature is measured using ruthenium oxide thermometers attached to a Fabry–Pérot resonator (FPR). The resonator frequency can be changed by changing the distance between the two mirrors [9]. DNP enhanced NMR or electron-nuclear double resonance experiments can be carried out with an FPR, though the double resonance experiments will be reported elsewhere. Figure 2 shows a schematic and a photograph of the FPR. The upper and lower parts of the FPR are a spherical and a flat mirror, respectively. The incident millimeter waves pass through the iris (coupling hole with 0.55 mm in diameter) and reflect between the mirrors, forming TEM_{00q} resonant modes, where q is an integer. The measurable temperature range extends down to 90 mK.

In order to evaluate the developed system, we employ two samples often used as standard samples of ESR [10]; $Mn_xMg_{1-x}O$ in which Mn^{2+} is diluted in nonmagnetic MgO, and an organic radical crystal DPPH which has a radical of $S = 1/2$ (a powder sample, contains 10-20 % benzene, manufactured by Tokyo Chemical Industry). An isolated Mn^{2+} ion (for which the outermost electron is in the $3d^5$state) has an ESR spectrum that is split into six components, which is known as its "hyperfine structure." This splitting is caused by the interaction of the isolated Mn^{2+} ion with the ^{55}Mn nuclear spin ($I = 5/2$). For this reason, a sample containing Mn^{2+} ions diluted in a nonmagnetic substance is useful as a magnetic-field marker [10-12], and $Mn_xMg_{1-x}O$ is thus used as such a marker in commercially available ESR apparatus. For $Mn_xMg_{1-x}O$ samples where x is sufficiently small (so that the spin interaction is small), it is expected that magnetic correlations will not develop at extremely low temperatures. Therefore, the detection sensitivity can be determined from the intensity of the ESR signal at cryogenic temperatures. We prepare a sample of $Mn_xMg_{1-x}O$ ($x = 1.0 \times 10^{-4}$) by first weighing the MgO and MnO to achieve the desired molar ratio and then heating the appropriate mixture in an electric furnace at approximately 1000 °C for 72 hours. Using a powder X-ray diffraction apparatus, we confirm that the crystal structure of the sample is that of MgO.

DPPH is well known as a standard sample of ESR [13]. However, magnetic properties at low-temperature region strongly depend on its crystal solvents [14-18]. It is important to investigate commercially available DPPH for further analyses at very low temperatures. We acquire fine powder of DPPH by grinding tiny crystals in order to obtain powder average of anisotropic g-value of DPPH. The powder DPPH is mixed with Apiezon N grease (M&I Materials) and put on the surface of the spherical mirror as shown in Figure 2. A amount of heat generated around the sample is estimated by the following simple consideration: The attenuation of the electromagnetic wave from the oscillator output (~10 mW at maximum) to the entrance of the resonator is approximately 40 dB. Thus, in each mirror of the resonator, a caloric value of 0.5 μW will be generated at maximum. We consider that this value is sufficiently small to avoid significant temperature rise of the sample.

3. Results and discussions

The distance from the iris to the flat mirror have fixed at 10 mm, which corresponds to the TEM_{007} mode for a Gaussian beam. As shown in Figure 2 (b), we affix a 10.8 mg sample of $Mn_xMg_{1-x}O$ to the center of the plane mirror. The $Mn_xMg_{1-x}O$ sample and the DPPH sample were separately positioned at the center of the superconducting magnet by raising and lowering the D/R probe and measuring the field strength. Figure 3 shows the ESR magnetic field as a function of D/R main body height for the two samples of $Mn_xMg_{1-x}O$ and DPPH. Here, data for the lowest field line 'Mn_{1st}' among the six lines of $Mn_xMg_{1-x}O$ are plotted. Each sample is at the center of the magnet when the resonance field takes minimum. The magnetic field strength profile is approximately parabolic near the center. It is natural that the difference of the positions that give the minimum resonance fields for the two samples are 10 mm distant from each other reflecting on the vertical distance between the samples as shown in Figure 2 (a).

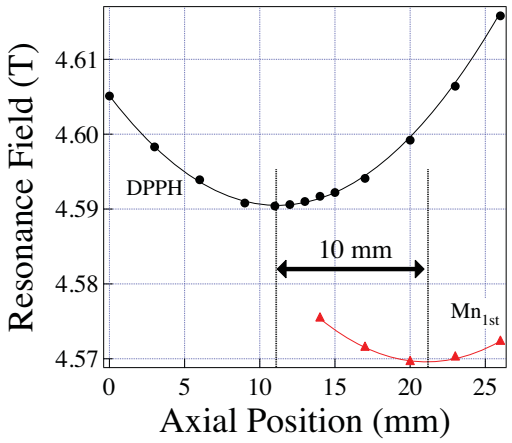

Figure 3. Magnetic-field measurements for DPPH and for the Mn_{1st} signal (see definition below) in $Mn_xMg_{1-x}O$ as functions of the position of the D/R probe along the magnetic field axis. Observed resonance fields where the ESR line for DPPH and $Mn_xMg_{1-x}O$ appear as functions of axial position of the sample. Each sample is located at the center of the magnet when the field is a minimum. Each parabolic line shows the fitting result to experimental plot.

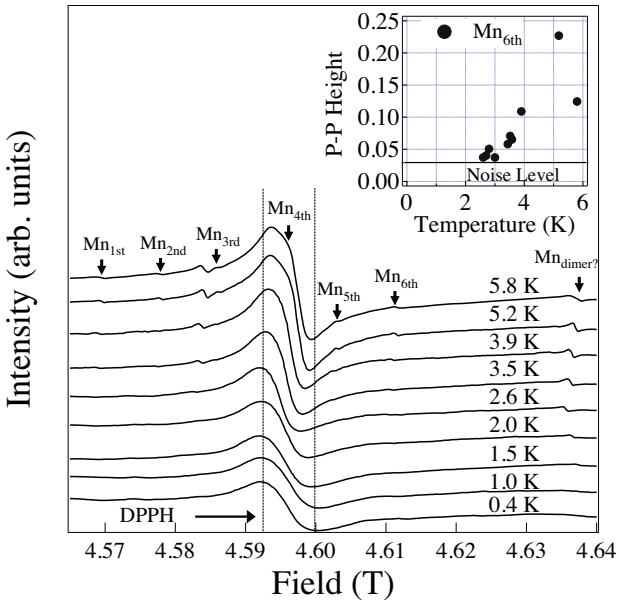

Figure 4. Temperature dependence of the dispersion signal of $Mn_xMg_{1-x}O$. The large central resonance line is from the DPPH radical in the FPR. The inset shows temperature dependence of the intensity (peak-to-peak height) of the Mn_{6th} signal.

Figure 4 shows the temperature dependence of the ESR spectrum of $Mn_xMg_{1-x}O$. At 5.8 K, we can identify six dispersion curves due to Mn^{2+}. Moreover, we label them as Mn_{1st} through Mn_{6th} in the order of increasing magnetic–field strength. These signals are separated from each other by approximately 420 Oe; this interval is due to the hyperfine structure and is consistent with the previously reported value [11, 12]. Although these ESR signals are observed at 5.8 K, they gradually decrease in amplitude as the temperature is lowered and disappear completely at 0.4 K. Here, the peak-to-peak (P-P) width is defined as the width of peak to peak of dispersion signal. Figure 4 inset shows the temperature dependence of the signal intensity (peak-to-peak height) of the dispersion curve with focusing on the Mn_{6th} signal. The signal intensity gradually decreases below 5.8 K and becomes invisible below 2.5 K. This is probably because the Mn^{2+} ions are not isolated sufficiently in the sample; therefore, correlations between relatively close ions develop at low temperatures. We determin the ESR detection sensitivity, define as the number of spins observable per Oe, from the Mn_{6th} signal at 5.8 K. ESR signal of unknown origin is detected around 4.365 T. This is likely to be a contribution from Mn – Mn dimer [19]. Here, the sensitivity of our device is estimated on the premise that all of the Mn of the sample are detected in the hyperfine split six ESR lines. The number of Mn^{2+} spins in the 10.8 mg sample of $Mn_xMg_{1-x}O$ ($x = 1.0 \times 10^{-4}$) is 1.0×10^{16}. Because the Mn^{2+} signal is divided into six spectra, the total number of spins must be divided by six. The P-P width of Mn_{6th} is 11 Oe and the S/N ratio is 4, the detection sensitivity is 6×10^{13} spins/G. We consider this value to be a

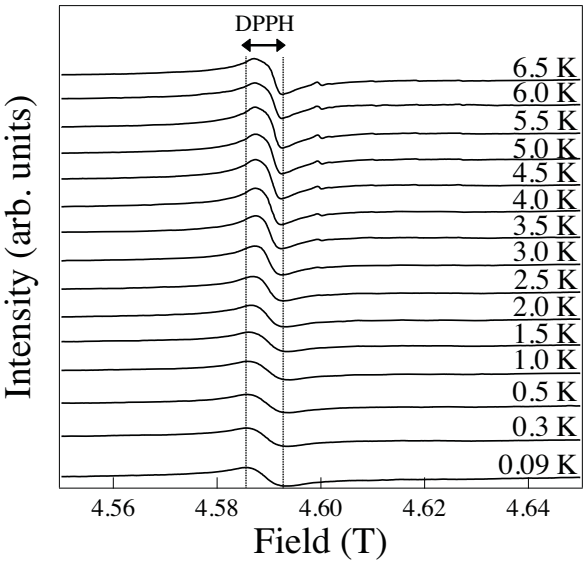

Figure 5. Dispersion of ESR signals from DPPH between 6.5 and 0.09 K. Signals from the $Mn_xMg_{1-x}O$ sample in the FPR are also observed.

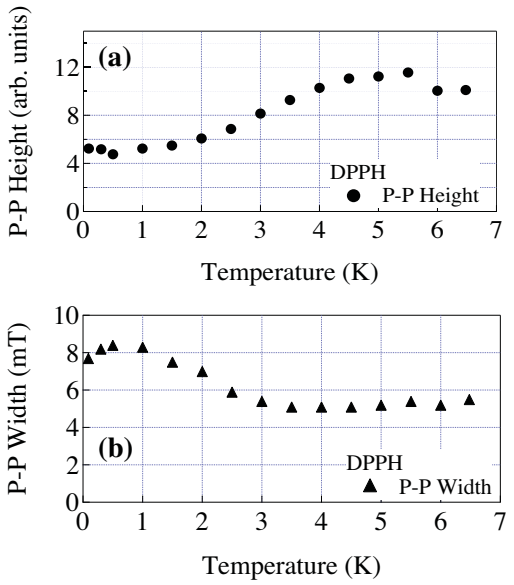

Figure 6. Temperature dependence of (a) the signal intensity (peak-to-peak height) and (b) peak to peak width of the ESR spectra of DPPH.

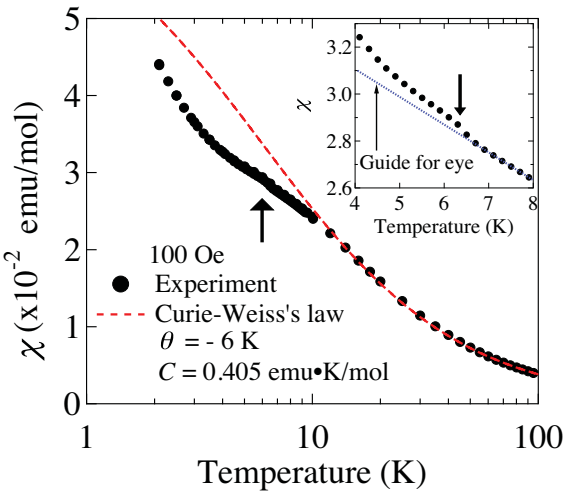

Figure 7. Temperature dependence of the magnetic susceptibility of DPPH. The arrow indicates an anomaly around 6 K. The inset shows the expansion below 8 K. The blue dot line shows Curie-Weiss's law $\chi = C / (T - \theta)$

lower limit to the actual sensitivity. Further experiments are necessary for more accurate quantitative discussion.

We conducted measurements on the DPPH sample over the temperature range of 6.5 – 0.09 K. As shown in Figure 5, the spectra clearly change over this temperature range. The changes in P-P width and signal intensity are complicated, as shown in Figure 6. We observe small anomalies both in the P-P width and the intensity near 6 K. As the temperature decreases below 3.5 K, the P-P width gradually increases, and the intensity decreases. Below approximately 0.5 K, the P-P width again decreases. We also measure the magnetic susceptibility χ of a 6.7 mg DPPH-powder sample in an applied magnetic field of 100 Oe by using the superconducting quantum interference device (SQUID) magnetometer (MPMS, Quantum Design) in the temperature range of 2 – 100 K. Results are shown in Figure 7. The susceptibility deviates from high-temperature Curie-Weiss type behavior below around 20 K, suggesting development of short-range antiferromagnetic ordering. We also have found a tiny

anomaly in the susceptibility around 6 K. This anomaly possibly corresponds to small change of ESR intensity from DPPH at 6 K shown in Figure 6 (a), though its origin is unclear so far. Considering that low-temperature behavior of ESR spectrum related with the development of magnetic correlations in this material differs depending upon the type of solvent used [13-18], it is important to analyze crystal structures of our DPPH with benzene. Nevertheless, the observed ESR spectrum of our DPPH shows almost no shift in the resonance position over the temperature range of 6.5 – 0.09 K, although the P-P width increases by about a factor of 1.5. We therefore consider DPPH to function as a useful standard sample with a magnetic-field accuracy of a few tens of gauss over this temperature range.

4. Summary

We have performed ESR measurements on $Mn_xMg_{1-x}O$ ($x = 1.0 \times 10^{-4}$) and DPPH at approximately 128 GHz over the temperature range of 0.09 – 6.5 K by using a millimeter-wave ESR apparatus developed for DNP-NMR measurements. At 5.8 K, we can identify six dispersion curves due to Mn^{2+}. ESR signals from Mn^{2+} gradually decrease in amplitude as the temperature is lowered and disappear completely at 0.4 K. This is because the Mn^{2+} ions are not isolated sufficiently. This behavior is likely to be a contribution from Mn-Mn dimer. From the ESR signal due to Mn^{2+} ions at 5.8 K, we also estimate the detection sensitivity of the ESR apparatus to be 6×10^{13} spins/G. In ESR measurements on DPPH, we have observed small anomalies around 6 K. We also have found a tiny anomaly in the susceptibility around 6 K. This anomaly possibly corresponds to small change of ESR intensity from DPPH. As the temperature is lowered near 3.5 K, the ESR P-P width gradually increases, while the signal intensity decreases. The P-P width decreases again at 0.5 K, and the signal intensity becomes constant. Because no shift in the resonance position was found over this temperature range, we consider that DPPH can be used as an ESR magnetic-field marker over the temperature range covered by our D/R experiments.

Acknowledgments

This work is partly supported by JSPS KAKENHI Grant Number 17K05514 and 26400331 and by the Cooperative Research Program of Research Center for Development of Far-Infrared Region, University of Fukui (No. H27FIRDM011E, H28FIRDM024A, H29FIRDM015B).

References

[1] Abragam A 1961 *The Principles of Nuclear Magnetism* (Oxford: Clarendon Press) chapter 9-10
[2] Kane B E 1998 *Nature* **133** 393
[3] Song M *et al*. 2010 *J. Phys.: Condens. Matter* **22** 206001
[4] Fujii Y *et al*. 2015 *J. Phys.: Conf. Series* **568** 042005
[5] Järvinen J *et al*. 2014 *Phys. Rev.* B **90** 214401
[6] Järvinen J *et al*. 2015 *Phys. Rev.* B **92** 121202
[7] Sakon T *et al*. 2003 *J. Phys. Soc. Jpn* **72** 140
[8] Smirnov A I *et al*. 2012 *Phys. Rev. B* **85** 184423
[9] Kogelnik H and Li T 1966 *Proc. IEEE.* **54** 10
[10] Smith G M and Riedi P C 2000 Progress in high field EPR *Electron Paramagnetic Resonance* vol 17, ed Gilbert B C *et al*. (Cambridge: The Royal Society of Chemistry) chapter 6, p 178
[11] Miner G K *et al*. 1972 *Rev. Sci. Instr*. **43** 1297
[12] Ohya H and Yamauchi J 1989 *Electron Spin Resonance* (in Japanese) (Tokyo: Kodansha) p 43
[13] Krzystek J *et al*. 1997 *J. Magn. Reson*. **125** 207
[14] Žilić D *et al*. 2010 *J. Magn. Reson*. **207** 34
[15] Fujito T 1981 *Bull. Chem. Soc. Jpn*. **54** 3110
[16] Prokhorov A M and Fedorov V B 1963 *Soviet Physics JETP* **16** 1489
[17] Voesch W *et al*. 2015 *Physics Procedia* **75** 503
[18] Teitel'baum G B *et al*. 1981 *JETP Letters* **34** 555
[19] Coles B A *et al*. 1960 *Phys. Rev. Lett* **4** 3